Signatures of Precocious Unification in Orbiting Detectors

G. Domokos and S. Kovesi-Domokos
Department of Physics and Astronomy
The Johns Hopkins University
Baltimore, MD 21218*
and
William S. Burgett and Jason Wrinkle
Department of Physics
University of Texas at Dallas
Richardson, TX 75083†

Revised version.

Abstract

It has been conjectured that the string and unification scales may be substantially lower than previously believed, perhaps a few TeV. In scenarios of this type, orbiting detectors such as OWL or AIRWATCH can observe spectacular phenomena at trans-GZK energies. We explore measurable signatures of the hypothesis that trans-GZK air showers ("anomalous showers") are originated by strongly interacting neutrinos. The results of a MC simulation of such air showers are described. A distinction between proton induced and "anomalous" showers is possible once a substantial sample of trans-GZK showers becomes available.

PACS: 12.10.Dm, 11.10.Kk, 14.60.St, 98.70.Sa

*e-mail: skd@jhu.edu
†e-mail: burgett@utdallas.edu

1 Introduction

The existence of trans-GZK cosmic rays is now reasonably well established: various detectors such as Fly's Eye, Agasa, and HiRes have collected over 20 events with primary energy exceeding 10^{20}eV. Based on present flux estimates, new experiments such as OWL, AIRWATCH, and the Pierre Auger observatory are expected to collect a total of over 10^3 events/year in this energy range.

The existence of trans-GZK events is a major puzzle since no source of such energetic particles has been plausibly identified within a distance of about 50 Mpc from the solar system. A brief summary of attempts to identify sources of trans-GZK events can be found in a recent review of Sigl[1].

In previous work we have conjectured that neutrinos of energy $E_0 \sim 10^{20}$ eV may acquire a strong interaction at the CM energies of the collision with an air nucleus while penetrating the CMBR essentially uninhibited [2, 3, 4]. Here, we summarize the essential features of this scenario. Consistency of string models requires that the strings "live" in a spacetime of dimension higher than the observed macroscopic spacetime (typically, $d \geq 10$). It has been observed that in such a situation the characteristic string scale M_s and the (*macroscopic*) Planck scale need not be the same, see [5, 6, 7][1]. In fact, the string scale can be considerably lower than the macroscopic Planck scale, perhaps of the order of 10 TeV or so. The exact relationship between the fundamental string scale and the macroscopic Planck scale depends on how one hides the extra dimensions. For example, one can think of compactified extra dimensions (as in ref. [5, 6]) or of a Randall-Sundrum mechanism [8].

The transition from the Standard Model regime to the regime governed by string physics is likely to be fast due to the rapidly rising level density in a string model [4]. There is a large degree of uncertainty in the details of such models. In particular, the characteristic energy scale (the string scale) can lie anywhere between a few TeV to perhaps a few hundred TeV. Hence, an analysis of experimental/observational data exploring these ideas has to satisfy the following criteria:

- It should concentrate on identifying the most robust features of models incorporating new ("stringy") physics; details vary from model to model, and it is difficult to foresee how a future more

[1]Due to to the large body of literature on the subject, we cite only the first works of the relevant authors on this topic.

complete theory will appear. Nevertheless, abstracting the important features of presently existing models provides guidance for future observations.

- Due to the uncertainty in establishing the characteristic energy scale, and recalling that the CM energy is in the range of a few hundred TeV for the trans-GZK events, it is necessary to investigate ultra-high energy cosmic ray (UHECR) data in addition to data from accelerator experiments. In developing new experiments for collecting UHECR data, the currently preferred detection system is an orbiting detector such as OWL or Airwatch because of the large target area available for observation as well as the capability to track the complete evolution of an atmospheric shower.

The approach adopted for this study was based on the following two main assumptions.

- The string and unification scales are close to each other or are equal. We denote the characteristic energy scale governing the onset of the string regime by $\sqrt{S}$. Due to uncertainties in model building at present, we set $S \approx M_s^2 \approx 1/\alpha^{'}$, thus ignoring a string coupling constant of order 1, and where $1/\alpha^{'}$ is the inverse Regge slope of the string model related to the string tension in the usual manner.
- Due to the excitation of the string degrees of freedom, there is a rapid transition between the regime where physics is described by the Standard Model and the string regime with unified interaction strength.

A detailed investigation of the sensitivity of MC simulations to particle physics uncertainties was carried out by Mikulski [9]. He found that for the case discussed here, the shower profiles and the fluctuation pattern are insensitive to the precise form of the transition between the Standard Model and string regimes, as well as to the precise form of the level density in the transition regimes, as long as the latter was a rapidly (typically, exponentially) rising function of $\sqrt{s}$.

In what follows, we provide an overview of the ALPS Monte Carlo simulation and the theoretical modeling used to obtain the results. The last section summarizes the key points of the work with an emphasis on the relevance to future orbiting detector experiments.

2 The simulation and its results

2.1 The ALPS simulation

A detailed description of the ALPS (Adaptive Longitudinal Profile Simulation) Monte Carlo program created by Mikulski is contained in ref. [9]. ALPS simulates the longitudinal development of a shower, and this is adequate for the high energies used in this study. A particularly useful feature of ALPS is its relatively fast execution time to generate air shower histories. It is easily modified to accept user-defined input physics beyond the Standard Model, and is adaptable as a front end generator to detector Monte Carlo simulations. ALPS is already being used by members of the OWL collaboration for cosmic ray signal and detector characterization.

More specifically, the starting point for the hadronic cascades is Approximation A, *i.e.*, the interaction length is independent of energy, and the inclusive cross section is dependent only on the ratio of outgoing particle energy to incident particle energy (Feynman scaling). In general, particles created in an air shower are simulated and tracked until their energy falls below a user-defined threshold (set to 1/1000 of the incident primary energy for this study) after which subshower parameterizations are introduced. The distribution of particles produced in the cascade below the above mentioned threshold is represented by a modified Gaisser-Hillas distribution. Corrections due to nuclear target effects and scaling violations are introduced both in the simulation and in the parameterized subshowers. The fitting parameters in the profile are dynamically adjusted by the program to satisfy goodness-of-fit criteria based on tracking selected subshowers. The electromagnetic cascades are implemented using a modified Greisen parameterization algorithm. Finally, there is a correction for the reduction of the bremsstrahlung and pair creation cross sections due to multiple scattering in the atmosphere (the Landau-Pomeranchuk-Migdal or LPM effect).

2.2 Theoretical considerations and modeling

For the purpose of exploring the conjectured "new physics" described in ref. [4], it was assumed that as long as $\sqrt{s} \geq \sqrt{S} \approx M_s$, an interaction produces an equal number of leptons and quarks. Once the primary energy falls below the string scale, $\sqrt{S}$, the shower evolves according to Standard Model physics. It was found that a step function-like onset

of the precociously unified physics gives a description indistinguishable from an exponentially rising level density which for $\sqrt{s} \gg M_s$ levels off due to unitarity corrections[2]. Hadronization of the quarks both in the string and Standard Model regimes is assumed to be consistent with a conventional splitting algorithm. Due to uncertainties in the models, at present no predictions can be made about how fast the various coupling constants are running with energy, but it is expected that they change faster than in the Standard Model [7]. The exact functional forms of the β functions in the renormalization group (RNG) equations that determine the energy scaling of the coupling constants depends on the spectrum of Kaluza-Klein excitations and on the specific string theory. For this reason, we extrapolated the strong cross sections into the energy range of $\sqrt{s} \approx 500$TeV using the fit of Block *et al.* [11], and set the cross section in the string regime to half of that value, due to uncertainties in the extrapolation. We prefer to err on the conservative side. Again, the results do not depend critically on the precise magnitude of the cross section in the string regime.

Relative multiplicities follow from the above assumption that any particle produced has a 50% probability of being a lepton or quark as long as the energy is larger than $\sqrt{S}$. Once energies fall below the characteristic scale, lepton interaction produces a multiplicity of 2 (counting leptons and photons on an equal footing), whereas a quark, after hadronization, produces high multiplicities in each interaction. At the energies considered here, a muon emits a bremsstrahlung photon almost at the same rate as an electron. Consequently, there is an excess of the low multiplicity component in the "anomalous" shower (*i.e.*, generated by a neutrino with precociously unified interactions). This contrasts with proton induced showers where the source of the leptonic component is the decay, $\pi^0 \to \gamma\gamma$. At the present level of accuracy, photoproduction of pions and other mesons can be neglected.

2.3 Average shower properties

The average profiles used for this study were derived such that shower development could be characterized independently of the relative po-

[2]Strictly speaking, a θ-function step in the cross section violates unitarity, since the real part of the forward elastic amplitude develops a logarithmic singularity. However, any smoothing of the θ-function removes the singularity and unitarity can be restored. There is no harm done if a step function is used in the total cross section: the latter depends on the imaginary part of the amplitude only.

sition with respect to the detector. Thus, the impact parameter b is selected to parameterize the geometry of the shower. Recalling that b is the distance of closest approach of the shower axis measured from the center of the Earth, we present results only for $b > R_\oplus$. Then, writing $b = R_\oplus + h$, the altitude h is the distance of closest approach measured from the surface of the Earth. Horizontal distances parameterizing the longitudinal shower development are defined to be measured along the shower axis, taking the point of closest approach as zero distance. Since all relevant showers take place in the upper atmosphere, an exponential atmosphere was used with a scale height of $h_0 = 6.4$ km yielding an adequate approximation to Shibata's parameterization [10].

The average shower profiles shown in Figure 1 are for $E_0 = 10^{20}$ eV proton and neutrino primaries incident on air nuclei (corresponding to $\sqrt{s} \approx 400$ TeV). The neutrino primaries are then "strongly interacting neutrinos" for precocious unification thresholds below $\sqrt{S} \sim 400$ TeV. As an example, the neutrino induced anomalous showers shown here were generated for $\sqrt{S} = 30$ TeV and $\sigma_\nu = \sigma_p/2$. Figure 1(a) shows the two profiles as a function of column density while Figures 1(b-d) present the profiles as a function of altitude above sea level to explicitly exhibit atmospheric effects. There is considerable broadening in the shower development at higher altitudes due to the low density of air as is evident in the profiles at $h = 28$ km. As shown in Figure 2, the number of electrons at the shower maximum, $N_{max} \approx 3 \times 10^{10}$, is only weakly dependent on the precise value of the string scale.

2.4 Fluctuations in shower development

The average shower profiles displayed in Figure 1 for neutrino induced showers reveal an interesting feature when compared with the proton induced events. The multiplicity around X_{max} is about half of the value for the proton induced shower due to the unified forces allowing a substantial portion of the primary energy to be channelled into prompt lepton production with the lepton interaction cross sections and multiplicities being smaller than those for hadronic channels. Consistent with this picture is the result that the electron deficiency *increases* with *decreasing* $\sqrt{S}$: for a lower characteristic energy scale, the prompt lepton production due to unification occurs over a longer interval of the shower development after the first interaction.

Although the average profile of a neutrino induced shower is different from a Standard Model proton induced shower, it is hard to distinguish

between the two types on an event-by-event basis. While it is true that *on average* $N_{\max}$ in a proton induced shower is roughly 2-3 times as large as for a neutrino induced event, and the development of the neutrino induced showers is somewhat slower compared to those induced by protons, fluctuations are likely to smear out such differences in any given shower.

However, a statistical analysis of a sample of showers should reveal a significant difference between neutrino and proton induced showers. Qualitatively, an important shower property is that smaller cross sections and smaller average multiplicities in individual interactions lead to larger fluctuations in the shower development. This qualitative expectation is borne out by the simulation results. Figure 3 displays the distribution of the position of the shower maximum, X_{max}, for various values of the characteristic scale, $\sqrt{S}$. For comparison, the same distribution is shown for normal showers generated by protons in the absence of new physics. Clearly, the width of the distribution in X_{max} for all the showers containing precociously unified interactions is considerably larger than those induced by protons. This is more evident if one plots the second central moments of the distributions versus the mean X_{max} as in Figure 4: there are clearly two distinct regions for proton and neutrino induced showers in this parameter space. One also observes that given sufficient statistics, the distribution in X_{max} gives a hint about the magnitude of $\sqrt{S}$: lower characteristic energies give rise to longer tails in the distribution.

Preliminary calculations also indicate that variations of the cross section at unification do not greatly affect the qualitative features of the results presented here. For example, if the cross section at unification is assumed to be equal to the extrapolated hadronic value used in this paper, $\langle X_{max} \rangle$ gets somewhat closer to the value for proton induced showers, and the rms fluctuations about X_{max} also decrease. However, the shower does not become statistically equivalent to the proton case. The difference arises because after the first few interactions in the neutrino showers, aproximately half the energy is distributed among leptons, and when the energy drops below the string threshold, the leptons contribute to shower development through lower multiplicity interactions compared to the hadronic channels.

3 Discussion

We find that orbiting detectors (and to some extent, any detector of the Fly's Eye type) can yield information about the presence or absence of certain types of new physics in trans-GZK showers. Two features are important from this point of view:

- The detector has to collect a substantial sample of trans-GZK events, since the difference between proton and neutrino induced showers is not sufficiently large for a distinction on an event-by event basis. This is primarily due to the fact that at any reasonable value of $\sqrt{S}$, the physics of the shower eventually becomes dominated by "low energy" Standard Model phenomena, and, hence, the largest number of particles is generated in the latter regime of shower development. A particular advantage of orbiting detectors is the capability for observing showers at a broad range of impact parameters, thus allowing an estimate of the magnitude of the cross sections.

- It appears that the shower development is rather insensitive to finer details of the models discussed in this paper. This is actually fortunate given the theoretical uncertainties at the present stage of model building. It is not yet clear how the analysis of data can be refined until more detailed and experimentally constrained models become available. However, the analysis proposed here is apparently robust. Once a sample size of greater than $\sim$100 events with well-determined profiles becomes available, a statistical analysis will reveal the presence or absence of the new physics proposed here. This is illustrated in Figure 5 where an event size of about 100 already gives a clear distinction between proton and neutrino induced showers. The result does not vary dramatically with a further increase of the number of events measured. Although the mean X_{max} values for the neutrino events change by only about 1% between the 100 and 50,000 run sample sizes, the standard deviations, as expected, settle more slowly changing by about 10% from 100 to 50,000 runs. Thus, very large sample sizes are required to bracket final values of the standard deviations to better than 1%.

Acknowledgements

We thank John Krizmanic for several useful discussions regarding the design of OWL. In particular, our choice of the significant impact parameters was based on his estimate of the intensity of air fluorescence as a function of the height above the surface of the Earth. We are also indebted to Paul Mikulski for sharing his insight into the ALPS program he authored.

References

[1] G. Sigl, Science **291**, 73 (2001).

[2] G. Domokos and S. Nussinov, Phys. Lett. **B 187**, 372 (1987).

[3] G. Domokos and S. Kovesi-Domokos, Phys. Rev. **D 38**, 2833 (1988).

[4] G. Domokos and S. Kovesi-Domokos, Phys. Rev. Letters **82**, 1366 (1999), e-print [hep-ph/9812260].

[5] J. Lykken, Phys. Rev. **D54**, 3693 (1996), e-print [hep-th/9603133].

[6] I. Antoniadis, S. Dimopoulos and G. Dvali, Nucl. Phys. **B516**, 70 (1997), e-print [hep-ph/9710204].

[7] K.R. Dienes, E. Dudas and T. Ghergetta, Phys. Lett. **B436**, 55 (1998), e-print [hep-ph/9803466].

[8] L. Randall and R. Sundrum, Phys.Rev. Lett. **83**, 4690 (1999), e-print [hep-th/9906064].

[9] Paul T. Mikulski, Dissertation (unpublished) (2000). A copy of the dissertation in pdf format is available from the OWL website at http://owl.gsfc.nasa.gov/mikulski-thesis.pdf

[10] T.K. Gaisser, "Cosmic Rays and Particle Physics", Cambridge University Press, New York (1990). Sec. 3.5.

[11] M.M. Block, F. Halzen and T. Stanev, Phys. Rev. **D 62**, 077501 (2000).

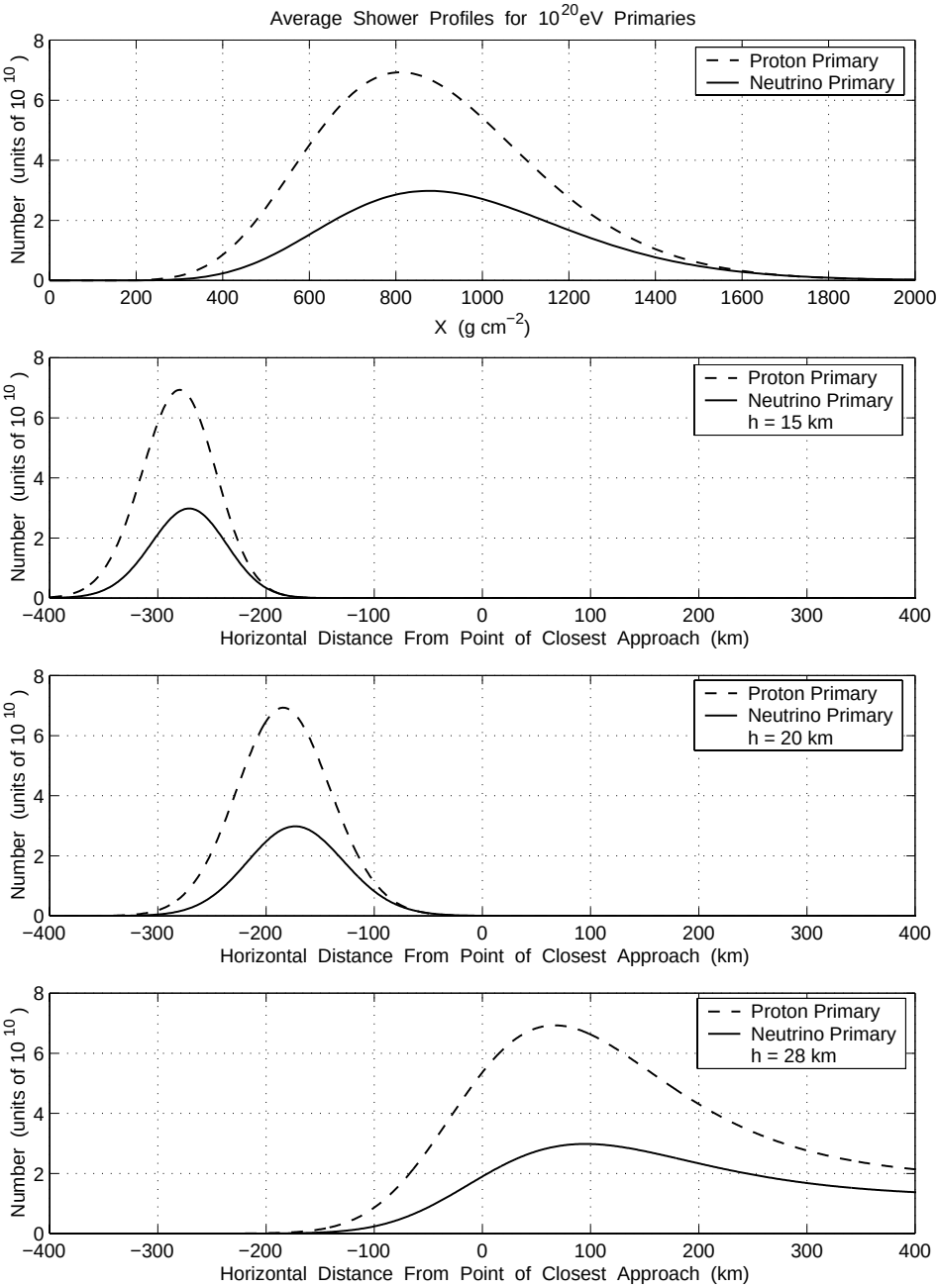

Figure 1: Comparison of average shower profiles for proton and neutrino induced showers as a function of column density and as a function of height above the Earth for a neutrino interaction cross section equal to half the proton value.

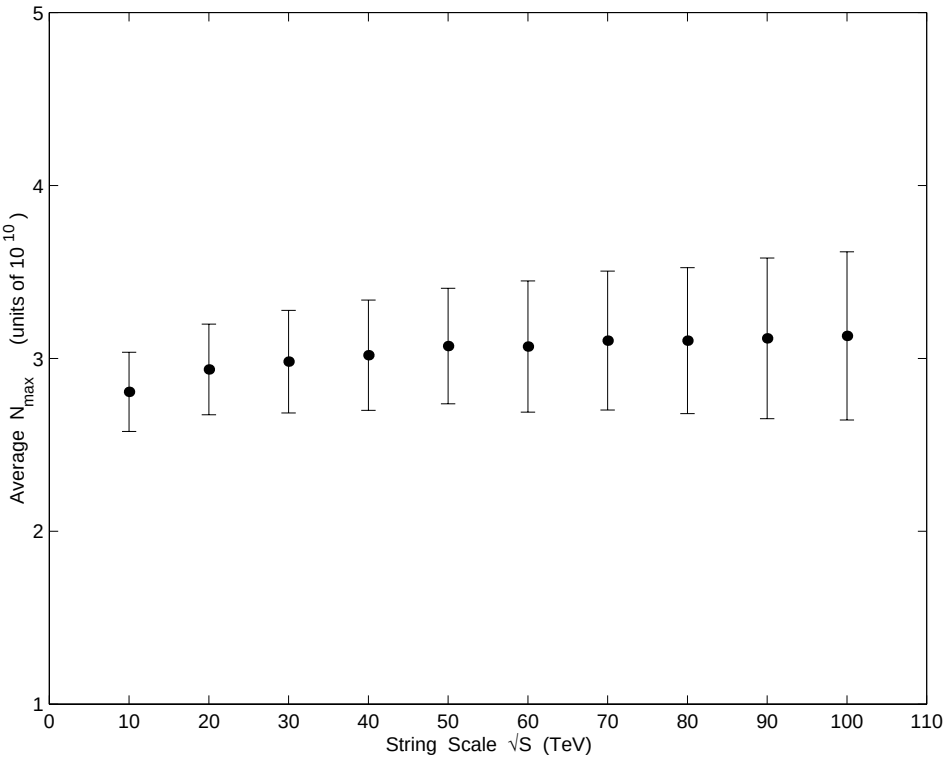

Figure 2: The number of electrons at shower maximum as a function of the string-motivated precocious unification scale $\sqrt{S}$ for a neutrino interaction cross section equal to half the proton value for sets of 1000 Monte Carlo runs.

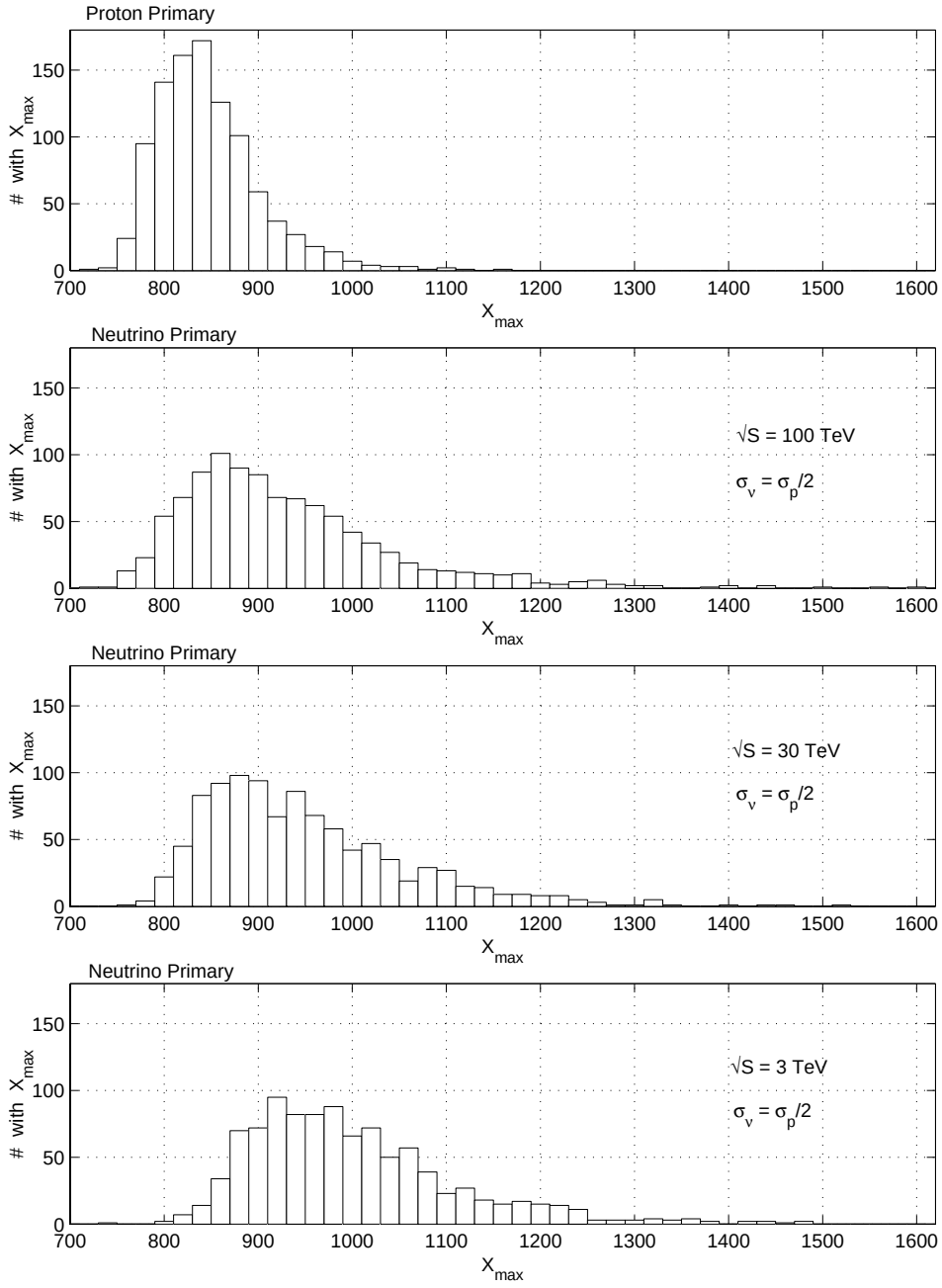

Figure 3: Distribution of shower maxima as a function of column density for precociously unified 10^{20} eV neutrino induced showers at 3 string scales compared to a conventional Standard Model 10^{20} eV proton induced shower.

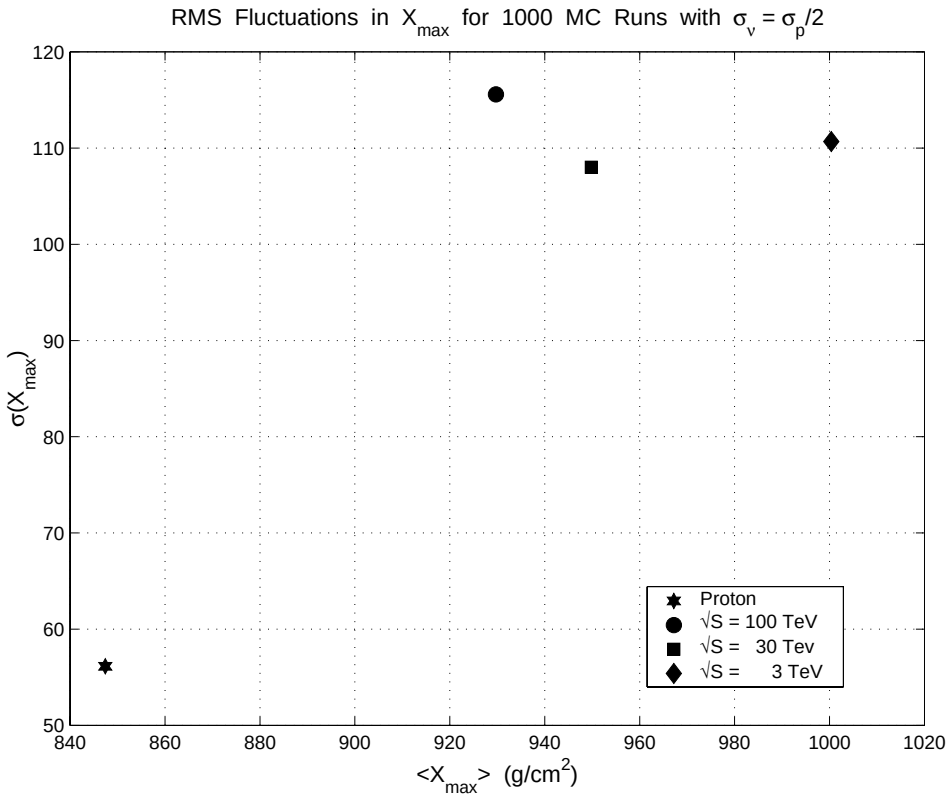

Figure 4: Standard deviations of the X_{max} distributions shown in Figure3 for proton and neutrino induced showers at various values of $\sqrt{S}$ and for a primary energy $E_0 = 10^{20}$ eV.

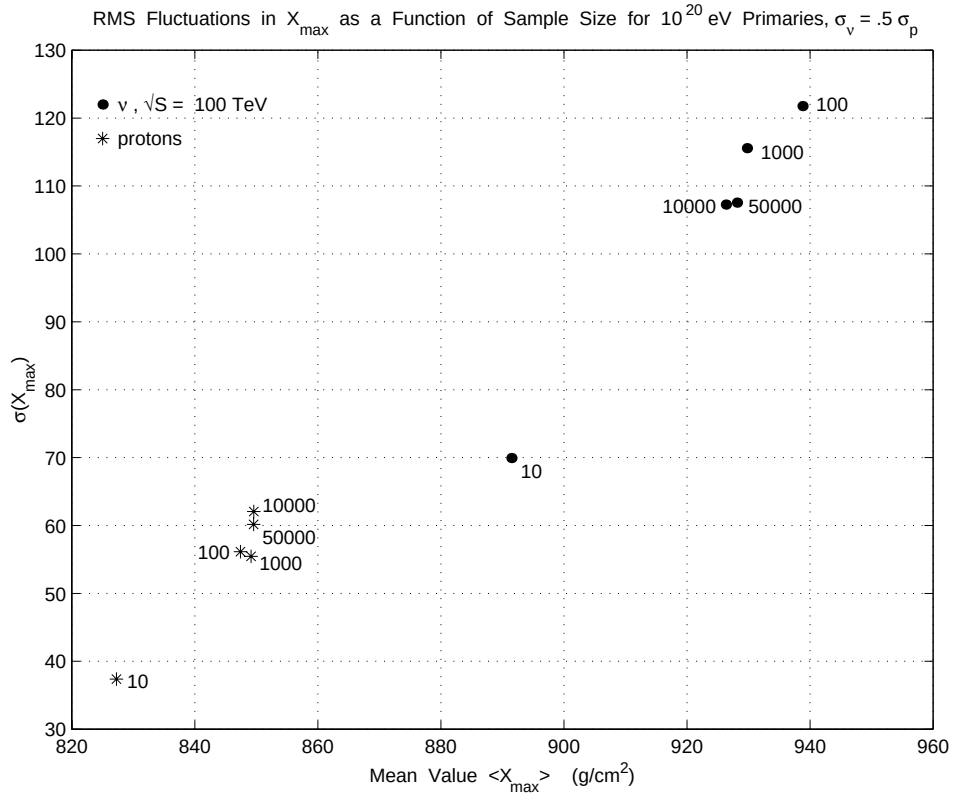

Figure 5: The measured standard deviations plotted against the average X_{max} for various sample sizes (the number adjacent to a data point indicates the number of MC runs over which averages were computed). Note that after only ~ 100 events, the average X_{max} and the standard deviation $\sigma(X_{max})$ converge to $\approx 1\%$ and 10% of their final values, respectively.